Characteristics of confinement and stability in large helical device edge plasmas[a)]

A. Komori,[b)] S. Sakakibara, T. Morisaki, K. Y. Watanabe, Y. Narushima, K. Toi, S. Ohdachi, S. Masuzaki, M. Kobayashi, M. Shoji, N. Ohyabu, K. Ida, K. Tanaka, K. Kawahata, K. Narihara, S. Morita, B. J. Peterson, R. Sakamoto, H. Yamada, K. Ikeda, O. Kaneko, M. Kobayashi, S. Kubo, J. Miyazawa, K. Nagaoka, H. Nakanishi, K. Ohkubo, Y. Oka, M. Osakabe, T. Shimozuma, Y. Takeiri, K. Tsumori, I. Yamada, Y. Yoshimura, M. Yoshinuma, and O. Motojima
(LHD Experimental Group)
National Institute for Fusion Science, Toki 509-5292, Japan

(Received 12 November 2004; accepted 2 March 2005; published online 28 April 2005)

Recent progress in the heating capability in the large helical device [O. Motojima *et al.*, Phys. Plasmas **6**, 1843 (1999)] has allowed the highest average β value (4.1%) obtained in the helical devices, and enables exploration of magnetohydrodynamics (MHD) stability in this β region. MHD activities in the periphery are found to become stable spontaneously from the inner region to the outer region when the averaged β value exceeds a threshold, and then a flattening of the electron temperature profile is observed around the resonant surface. Such a flattening can be formed externally by producing an $m/n=1/1$ magnetic island, and the complete stabilization of the $m/n=1/1$ mode is demonstrated by the moderate island width. In addition, attempts to control peripheral plasmas are also performed by using a limiter and a local island divertor utilizing the $m/n=1/1$ island, to improve plasma confinement and, especially, to stabilize pressure-driven modes in the present study. The stabilization of peripheral MHD modes is obtained with both approaches, and this indicates that these are available to the production of higher-β plasmas without edge MHD activities. © *2005 American Institute of Physics*. [DOI: 10.1063/1.1898227]

I. INTRODUCTION

The formation of steep pressure gradients in the edge region is one of major subjects in toroidal systems such as tokamaks and helical devices to produce high-β plasmas and to improve plasma confinement like in the *H* mode. This strongly depends on the growth of edge magnetohydrodynamics (MHD) activities. In tokamaks, the edge localized mode (ELM) affects maintaining the *H* mode and the available operation regime. The investigation of its physical mechanism and control has been continued for a long time through various experiments.[1] Net-current free plasmas in helical devices are free from current-driven instabilities unlike in tokamaks. The characterization of pressure-driven modes, especially, in the edge region, and their control in the high-β regime are the crucial issues towards a helical fusion reactor. Since the heliotron configuration has a magnetic hill in the peripheral region, the stabilization of ideal and resistive interchange modes is very important to produce the high-β plasmas. With regard to the modes at resonances in the core region, the stabilization due to the spontaneous generation of magnetic well has been verified in the experiment.[2] On the contrary, the theoretical prediction suggests that the low-*n* ideal instability such as $m/n=1/1$ mode that has a resonance around $\rho=0.9$ limits the pressure gradient in the peripheral region and, consequently, determines the β limit,[3] where *m* and *n* are the toroidal and poloidal mode numbers, respectively, and $\rho=(\Psi)^{1/2}$, where Ψ is the toroidal flux function, which is normalized by the value of the last closed flux surface. In the previous experiments, performed in the large helical device (LHD), the MHD modes excited in the peripheral region have been observed even in the low-β regime. The amplitude of the $\iota/2\pi=1$ resonant mode increases exponentially with β and the pressure gradient around the resonance in the $\langle\beta_{\mathrm{dia}}\rangle$ ranges up to 3.2%. In addition, the amplitudes of the modes excited outside the $\iota/2\pi=1$ resonance are considerably enhanced in the *H*-mode like plasma with the steep edge-pressure gradient.[4] Since there are the several low-*n* rational surfaces in the peripheral region, the relationship between the activities of their resonant modes and the pressure gradient is one of the key issues for higher-β plasma production. On the other hand, the plasma shifts due to the finite-β effects may result in the ergodization of magnetic surfaces and/or the generation of magnetic island, especially in the edge region. These might limit the plasma performance. An optimization of the magnetic configuration is required for the avoidance of β limits due to both stability and equilibrium. And also, it should be done for realizing good transport and high heating efficiency.

LHD has a heliotron-type magnetic configuration with a natural separatrix, and there is an ergodized layer around the separatrix. The magnetic configuration can be changed over a wide range by currents in the external helical and poloidal field coils. Also, LHD can have various magnetic configurations by using external perturbation coils located above and

[a)]Paper CI2A 3, Bull. Am. Phys. Soc. **49**, 59 (2004).
[b)]Invited speaker.

below the torus. A local island divertor (LID) is a powerful tool for the control of edge plasmas,[5] and fundamental divertor functions of the LID have been demonstrated in the recent experiments.[6,7] In the LID, the divertor head is inserted inside the O point of the $m/n=1/1$ magnetic island generated by the perturbation coils. This divertor head also works as a plasma limiter without generating the $m/n=1/1$ island, and these two approaches are available for the pressure-gradient control in the edge region.

Since LHD experiments started in 1998, plasma parameters have been improved with an increase in the heating power in every experimental campaign. In the recent experiments, the maximum averaged beta value, $\langle\beta_{\mathrm{dia}}\rangle$, of 4.1% was achieved by the high-power neutral beam heating of up to 12 MW in the magnetic configuration with relative high aspect ratio A_p, of 6.3.[8] Here $\langle\beta_{\mathrm{dia}}\rangle$ is defined as $4\mu_0/3W_{\mathrm{dia}}(B_{\mathrm{av0}}{}^2V_{p0})$, where W_{dia} is the diamagnetic energy. The B_{av0} and V_{p0} are averaged toroidal magnetic field inside the plasma boundary and plasma volume, respectively. They are estimated under the vacuum condition except for special configurations such as the limiter and LID. This paper describes recent experimental results on high-β plasmas, especially, edge MHD activities, and MHD characteristics in the limiter and LID configurations. In Sec. II, the magnetic configurations applied in the experiments are explained. Typical high-β discharges and the β dependence of MHD activities are shown in Sec. III. Section IV describes the observations of MHD modes in the limiter and LID configurations and the brief results of the LID experiments. The concluding remarks are shown in Sec. V.

II. MAGNETIC CONFIGURATIONS

The LHD is a heliotron-type device with a pair of continuous helical coils and three pairs of poloidal field coils, and these coils are superconductive. The magnetic axis position R_{ax}, can be changed from 3.4 to 4.1 m by controlling the poloidal coil currents, and it characterizes the transport and MHD stability. In the configuration with the inward-shifted R_{ax}, particle confinement is better than the outward-shifted case, because an effective helical ripple loss of neoclassical transport decreases. On the contrary, the inward-shifted plasma has a disadvantage with respect to MHD stability because of the magnetic hill formation. R_{ax} of 3.6 m was used in the high-β experiments, because the longest energy confinement has been obtained and serious MHD activities have not been observed in the previous experiments.[9] On the other hand, the LHD magnetic configuration also has a free degree of the aspect ratio to some extent. The helical coil consists of three layers, and by cotrolling the individual layer current, the aspect ratio of plasma, A_p, can be changed from 5.8 to 8.3 at $R_{\mathrm{ax}}=3.6$ m. Figure 1 shows the central rotational transform and effective plasma minor radius a_{eff} as a function of A_p. The large central rotational transform is expected to lead to the reduction of Shafranov shift, which restrains the degradation of heating efficiency of the neutral beam. Moreover, the large rotational transform contributes to the reduction of the helical ripple loss of high-energy particles. Although the reduction of the Shafranov shift obstructs the

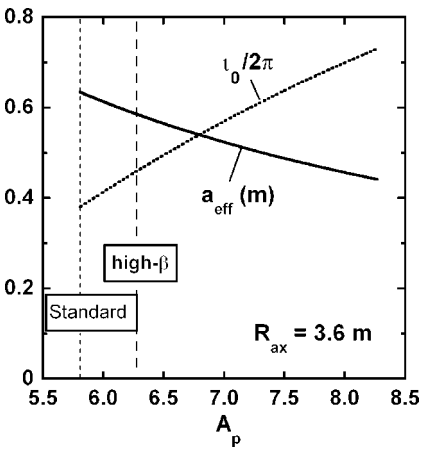

FIG. 1. Changes of a central rotational transform and an effective minor radius as a function of plasma aspect ratio.

magnetic well formation in the core region,[10] the resonant surface of the $m/n=2/1$ mode, which sometime affects the core pressure profile,[11] is expected to be eliminated due to the finite-β effect, because of the increase in the central $\iota/2\pi$. The aspect ratio, A_p of 5.8 was used in the high-β experiments up to now, and the complete optimization of A_p will be done in the next stage of the high-β experiment in LHD.

Figure 2(a) shows the schematic view of the LID. The LID is a closed divertor that utilizes an $m/n=1/1$ island generated in the edge region.[5] By inserting the divertor head into the island from the outer side of the torus, the outer island separatrix are interrupted by the divertor head. The particle and heat fluxes, diffused from the core plasma and crossing the inner island separatrix, flow along the inner separatrix of the island. After several toroidal turns, they reach the outer separatrix of the island, where the divertor head is placed, and strike upon its backside, on which they are neutralized and recycled, as shown in Fig. 2(a). Particles neutralized and recycled there are pumped out efficiently by a strong pumping system with a pumping duct designed to be a closed system. Since the blades of the divertor head are located inside the island separatrix, there is no leading edge problem. High efficient pumping is the key in realizing high temperature divertor operation, where the divertor plasma

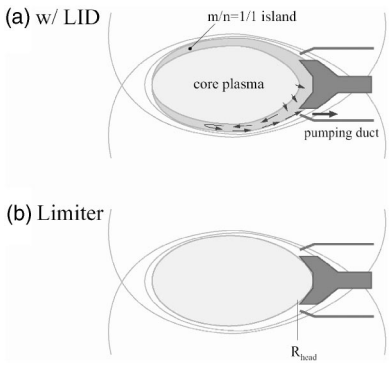

FIG. 2. Schematic view of (a) the local island divertor and (b) limiter configurations.

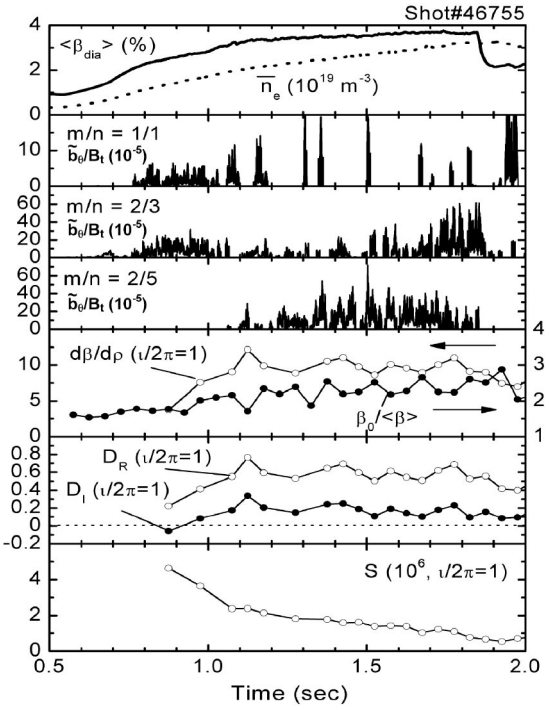

FIG. 3. Temporal changes of plasma parameters and MHD activities in typical high-β discharge.

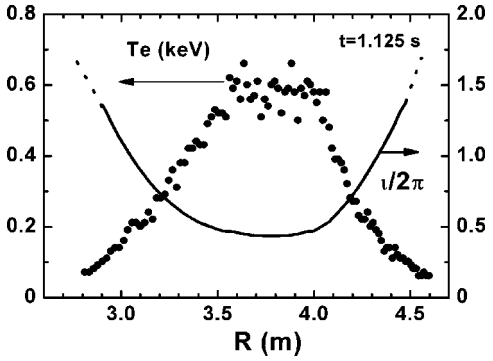

FIG. 4. Profiles of electron temperature and rotational transform at 1.125 s in the discharge shown in Fig. 3.

with a temperature of a few keV is produced, resulting in a significant improvement of energy confinement.[5] A closed divertor also provides high plasma plugging efficiency required for the high recycling operation, where a low temperature and high density divertor plasma is produced for radiative cooling. These two operational modes can be realized in the LID.[5] These divertor functions allow the LID to pump out ionized impurities that are difficult to be pumped out in the presence of the magnetic field. By using the divertor head alone, that is, without generating the $m/n=1/1$ island, the limiter configuration can be established, as shown in Fig. 2(b). In both configurations, the position of the divertor head is defined by the position of the blades of the divertor head along the major radius, as shown in Fig. 2(b).

III. HIGH-β EXPERIMENTS

Figure 3 shows MHD activities in the typical high-β discharge. R_{ax} and toroidal magnetic field B_t are chosen at 3.6 m and 0.5 T, respectively, and A_p is set at 6.3. Three neutral beams are injected to the plasma and the deposition power is about 6.9 MW at 1.725 s. The line averaged electron density $\overline{n_e}$, measured with the far infrared interferometer, gradually increases with time to 3.2×10^{19} m^{-3}. The $m/n=1/1$, 2/3, and 2/5 modes excited in the edge region are dominantly observed in this discharge. The $m/n=1/1$ and 2/3 modes grow from about 0.7 s and their amplitudes increase with $\langle\beta_{dia}\rangle$. However, when $\langle\beta_{dia}\rangle$ exceeds a threshold value at about 1 s, the $m/n=1/1$ mode becomes intermittent with a relative long interval and the amplitude of $m/n=2/3$ mode begins to decrease. At the same time, $\langle\beta_{dia}\rangle$ starts to increase, and the amplitude of the $m/n=2/5$ mode increases after the increase in $\langle\beta_{dia}\rangle$. At 1.73 s, the degradation of $\langle\beta_{dia}\rangle$ occurs with growth of the $m/n=2/3$ mode and the decrease in the $m/n=2/5$ mode amplitude, although the heating power and the supply of H_2 gas are still maintained. The equilibrium reconstruction and stability analysis are carried out for this discharge using the three-dimensional (3D) MHD equilibrium code VMEC,[12] and the result of $m/n=1/1$ mode is shown in Fig. 3 as an example. While the pressure gradient around the $m/n=1/1$ resonant surface increases with $\langle\beta_{dia}\rangle$ and saturates at 1.1 s, the peaking factor of pressure profile increases till one NBI is turned off at about 1.8 s. The Mercier parameter D_I, which is well used as an index of high-n ideal stability boundary, indicates that the high-n mode is unstable because of the reduction of magnetic shear due to finite-β effect. Plasmas are expected to be marginally stable on low-n ideal mode because D_I is around 0.2. The parameter D_R is an index of resistive interchange stability boundary, and positive D_R means the resistive mode is still unstable during the discharge. The magnetic Reynolds number S, which is related to the linear growth rate of resistive interchange mode,[13] decreases with an increase in $\langle\beta_{dia}\rangle$, and this suggests the gradual rise of the growth rate of the mode. These results seem to be inconsistent with the suppression of the $m/n=1/1$ mode. Figure 4 shows the radial T_e profile and rotational transform at 1.125 s, corresponding to the discharge shown in Fig. 3. The flattening structure is found in the radial T_e profile, for example, near the $m/n=1/1$ resonant surface. Since the measurement error of Thomson scattering system is ±5 eV in the R range of 3.0–3.2 m, the observed flattening structure is meaningful. These asymmetrical structures are well observed in the high-β discharges, and it is, however, difficult to apply such profiles to the present equilibrium reconstruction. The flattening is considered to contribute to the stabilization of both ideal and resistive modes. One possible way to form the asymmetrical profile in the periphery is to change the magnetic surfaces due to finite-β effect, for example, to generate the magnetic island. Therefore, the detail equilibrium reconstruction using the HINT code,[14] which can treat the configuration with magnetic islands, is desired in the near future for analysis.

Figure 5 shows the amplitudes of observed MHD modes as a function of $\langle\beta_{dia}\rangle$ at $A_p=6.3$. Although the $m/n=2/1$ mode in the core region has been observed in the $\langle\beta_{dia}\rangle$ range

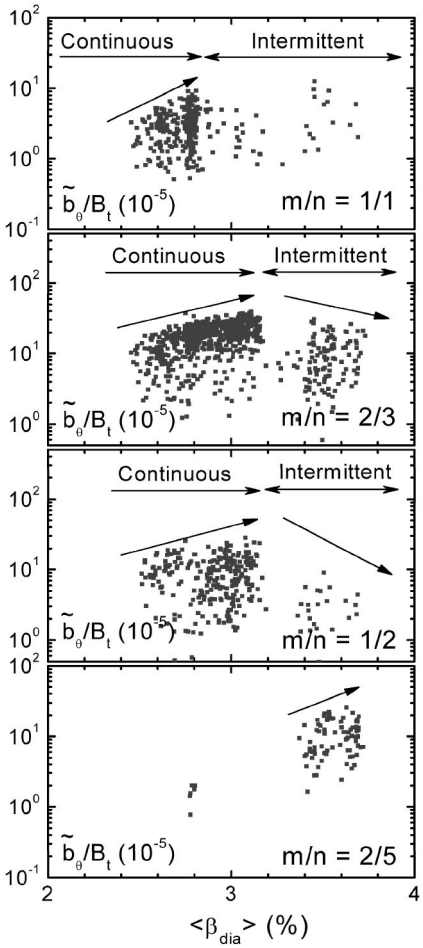

FIG. 5. Amplitudes of observed MHD modes as a function of $\langle\beta_{\rm dia}\rangle$.

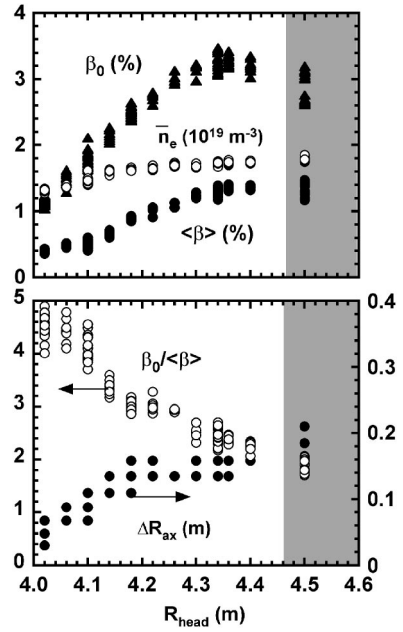

FIG. 6. Changes of central β_0, $\langle\beta\rangle$, $\beta_0/\langle\beta\rangle$, $\overline{n_e}$, and $\Delta R_{\rm ax}$ as a function of $R_{\rm head}$.

of less than 2.5% in the previous experiments, this mode disappears in the present experiments. The resonant surfaces with $\iota/2\pi \geqslant 1$ are located at $\rho \geqslant 0.9$ and their resonant modes are dominantly observed in the $\langle\beta_{\rm dia}\rangle$ range of more than 2.5%. At first the amplitude of the $m/n=1/1$ mode increases with $\langle\beta_{\rm dia}\rangle$, but it disappears or is intermittently observed when $\langle\beta_{\rm dia}\rangle$ exceeds 2.8%. Although the amplitudes of $m/n=2/3$ and $1/2$ modes change, being similar to that of $m/n=1/1$ mode, the threshold $\langle\beta_{\rm dia}\rangle$, where the mode is eliminated, is larger in the higher mode. The $m/n=2/5$ mode appears when $\langle\beta_{\rm dia}\rangle$ exceeds 3.4%, and its amplitude still increases with $\langle\beta_{\rm dia}\rangle$ in the present $\langle\beta_{\rm dia}\rangle$ range. These phenomena suggest that the "stable" region is expanded with $\langle\beta_{\rm dia}\rangle$ from the inner region to the outer one. The destabilization of the MHD mode just outside the stable region may be caused by the steep pressure gradient, formed outside the flattened profile, as it is shown in the T_e profile, especially, on the small-R side in Fig. 4, where the T_e gradient is steeper than that in the large-R side.

The shift $\Delta R_{\rm ax}$, of the magnetic axis position is obtained using the T_e profile, measured with Thomson scattering system, and is about 0.25 m at 1.725 s in the discharge shown in Fig. 3. This corresponds to $\Delta R/a \sim 0.25$. The statistical analysis indicates that this shift is smaller by about 50% than that of the standard LHD magnetic configuration with $A_p=5.8$. One reason for this is that the rotational transform at $A_p=6.3$ is larger than the standard case described in Sec. II, resulting in the restriction of Shafranov shift. Although the reduction of Shafranov shift limits the formation of magnetic well in the core plasma, it has the advantage of yielding the higher β limit resulting from MHD equilibrium. Also, it contributes to prevent the reduction of the heat deposition of neutral beams, because the direction of the neutral beams is optimized to the magnetic configuration with $R_{\rm ax}=3.6-3.7$ m. Therefore, the high-aspect-ratio configuration may be suitable for high-β plasma production from a viewpoint of the power deposition. On the other hand, the variation of magnetic field structure may be an essential issue for the production of higher-β plasma rather than the $R_{\rm ax}$ shift itself from a viewpoint of equilibrium β limit.

IV. EDGE MHD ACTIVITIES IN LIMITER AND LID CONFIGURATIONS

A. Limiter configuration

While the spontaneous suppression of peripheral MHD modes occurs in the high-β plasmas, the first attempt to stabilize the MHD instabilities by an active control of pressure gradient with the limiter has been done. Here, the divertor head was used as a limiter, as shown in Fig. 2(b), and it was inserted into the plasma at $R_{\rm ax}=3.6$ m, $B_t=0.75$ T, and $A_p=5.8$. The coneutral and counterneutral beams were injected into the plasma and the total deposition power was about 3 MW. Figure 6 shows the changes of plasma parameters as a function of $R_{\rm head}$. $\langle\beta_{\rm dia}\rangle$ and $\overline{n_e}$ at each $R_{\rm head}$ are compensated by using an effective plasma minor radii, $r_{\rm eff}$'s, as shown in Fig. 7. In the configuration without the limiter, that is, in the gray area in this figure, β_0 and $\langle\beta_{\rm dia}\rangle$ are about 3% and 1.3%, respectively. $\langle\beta_{\rm dia}\rangle$ and $\overline{n_e}$ have almost the same values in the $R_{\rm head}$ range above 4.34 m, and they start to

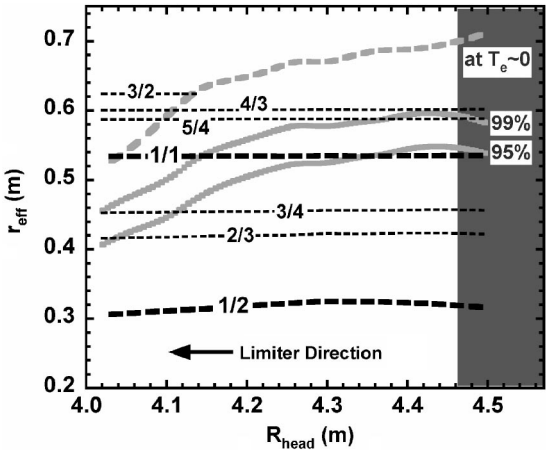

FIG. 7. Radial position of $T_e \sim 0$ eV, radial positions, inside which the electron stored energies are 95% and 99% of its total, respectively, and radial positions of several resonant surfaces, as a function of R_{head}.

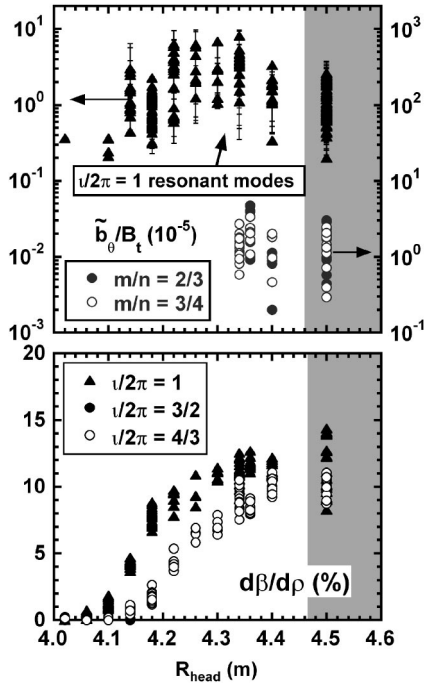

FIG. 8. Amplitudes of MHD modes excited at $\iota/2\pi = 1/q = 1$, 3/2, and 4/3 resonant surfaces and β gradients at each resonance, as a function of R_{head}.

decrease when the limiter was inserted into the plasma. Although β_0 increases at first by inserting the limiter up to 4.34 m, it decreases till the limiter reaches $R_{\text{head}}=4.02$ m. The peaking factor of β profile, $\beta_0/\langle\beta_{\text{dia}}\rangle$, continues to increase from 2 to 4.5 with the limiter inserting into the plasma. The Shafranov shift ΔR_{ax} keeps decreasing while inserting the limiter in spite of the increase in the peaking factor because of the reductions of β_0 and $\langle\beta_{\text{dia}}\rangle$. In these experiments, the degradation of plasma confinements with inserting limiter were observed, and we guess that this is due to the inflow of impurities recycled from LID head because radiation power increases with inserting limiter.

Figure 7 shows the radial position of $T_e \sim 0$ eV, obtained by using the T_e profile, the radial positions, inside which the electron stored energies are 95% and 99% of its total, respectively, and the several radial positions of resonant surfaces estimated by the VMEC code, as a function of R_{head}, where the electron stored energy is estimated by electron density profile measured with FIR interferometer and electron temperature profile by Thomson scattering system. In case of $R_{\text{head}}=4.02$ m, the plasma minor radius decreases by 24%, compared with that without the limiter. The positions of resonant surfaces depend weakly on R_{head} except for the $\iota/2\pi=1/2$ surface that is sensitive to the Shafranov shift. The radial position of $T_e \sim 0$ eV and the radial positions, inside which the electron stored energies are 95% and 99% of its total, respectively, move abruptly towards the plasma center when $R_{\text{head}}<4.24$ m. Note that the absence of an $\iota/2\pi=3/2$ surface is due to the difficulty of the equilibrium calculation in the plasma edge, although the resonance exists certainly because $\iota/2\pi$ at the natural separatrix is 5 in LHD.

Figure 8 shows the amplitudes of the $\iota/2\pi \geqslant 1$ resonant modes and β gradients at their resonances as a function of R_{head}. The amplitude of the $\iota/2\pi=1$ resonant mode grows at first with the β gradient by inserting the limiter, but then begins to be stabilized when $R_{\text{head}}<4.3$ m at the same time when the β gradient decreases. At $R_{\text{head}}=4.08$ m, which is the standard position in the LID experiments, the amplitude of the $\iota/2\pi=1$ resonant mode becomes very small. On the other hand, the $\iota/2\pi>1$ resonant modes are observed in the R_{head} range of $\geqslant 4.34$ m, and they are completely stabilized when $R_{\text{head}}<4.34$ m.

The $m/n=2/1$ mode excited in the core region grows with the increase in the peaking factor of pressure profile when the limiter is inserted, and it causes the flattening of the T_e profile around the resonance. However, the amplitude decreases abruptly when $R_{\text{head}}<4.14$ m, and the peaking factor increases once more, as shown in Fig. 6. One of the reasons for the stabilization is that the experimental conditions enter the stable regime of $\langle\beta_{\text{dia}}\rangle$ vs β gradient diagram, because of the decrease in $\langle\beta_{\text{dia}}\rangle$. The previous experiments show that the degradation of plasma confinement due to this mode is less than 10% even if it is such a strong mode that the pressure profile changes. Moreover, this mode is spontaneously stabilized due to the magnetic well formation in the high-β regime.

The results of the edge MHD activities, described above, suggest that the divertor head position of $R_{\text{head}}=4.3$ m is suitable for the suppression of the $\iota/2\pi>1$ modes, and no degradation of $\langle\beta_{\text{dia}}\rangle$ is observed with inserting the limiter. However, at this limiter position, the amplitude of the $\iota/2\pi=1$ mode is larger than that without the limiter by one order of magnitude, as shown in Fig. 9. This is because the steep β gradient is formed. Thus, the configuration with $R_{\text{head}}<4.14$ m is valid for suppression of core and edge MHD instabilities.

B. LID configuration

Another scheme for the active edge control is formed by using the LID. Figure 10 shows the typical radial profiles of (a) electron temperature $T_e(R)$, (b) I_{TS}, which is a rough measure of electron density n_e measured with the Thomson scat-

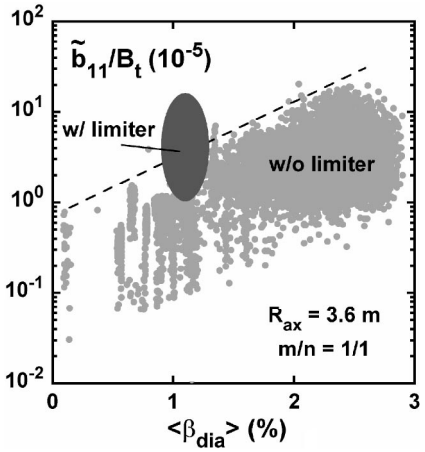

FIG. 9. Comparison between amplitudes of the $m/n=1/1$ mode in the limiter configuration with $R_{\text{head}}=4.3$ m and the standard configuration.

tering system, together with (c) the Poincare plot of the island separatrix at the toroidal position of the Thomson scattering measurement. It is clearly seen that T_e is bounded on the inner separatrix of the island. The I_{TS} profile is broader than the T_e profile. Namely, I_{TS} is bounded on the outer separatrix of the island and changes its gradient at the inner separatrix of the island. The relatively high density but low temperature plasma remains in the island region. The I_{TS} profile in the island shows a hollow shape, as shown in Fig. 10(b). The connection length of the magnetic field around the island, that is, from near the inner separatrix of the island on the equatorial plane to the divertor head is long enough for such low temperature plasmas to remain. The parallel transport is dominant. An interesting feature is also observed in the T_e profile, that is, small peaks exist at the outer separatrix of the island. Although another peak of the T_e profile at $R=4.5$ m appears, it is due to measurement error because it appears only at this time and consists of one data. These results indicate that the particle and heat fluxes are guided to the divertor head along the field lines. Furthermore the very steep gradient in the T_e profile is established, which is attributed to the improvement of local confinement in the edge region, compared with that in the standard LHD magnetic configuration.

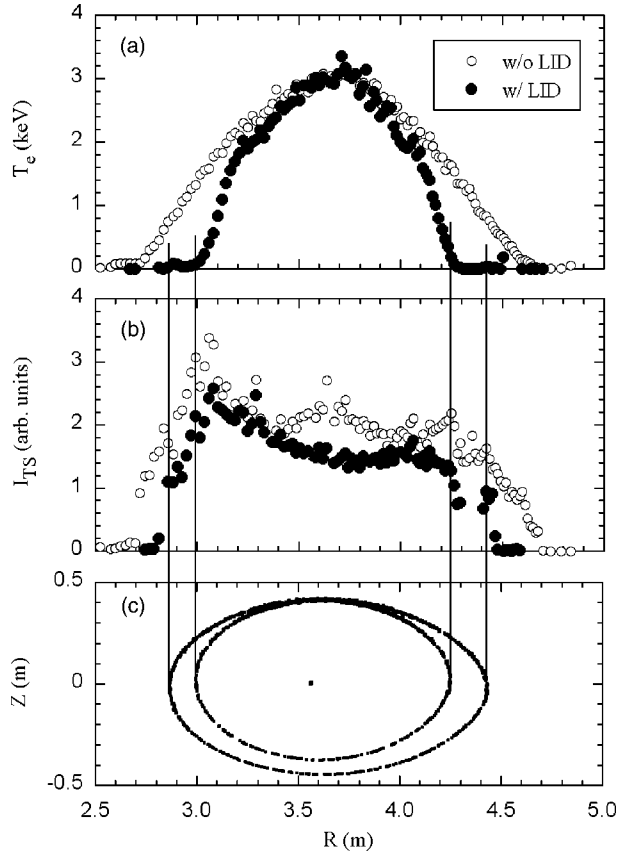

FIG. 10. Radial profiles of (a) electron temperature $T_e(R)$, (b) a rough measure of electron density, I_{TS}, together with (c) the Poincare plot of the island separatrix at the Thomson scattering location.

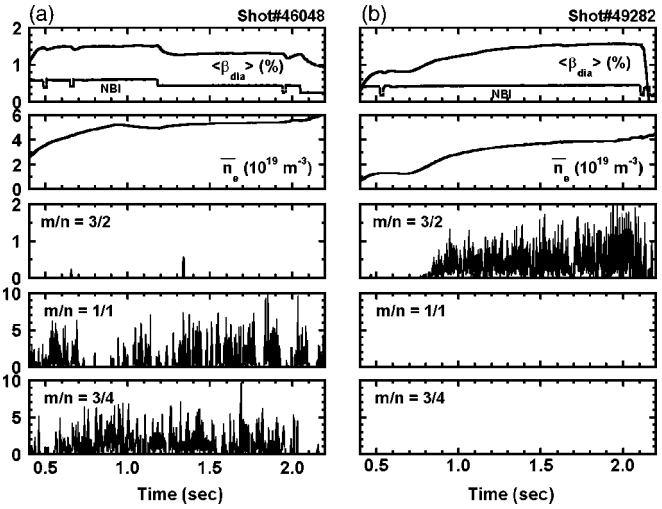

FIG. 11. MHD activities in (a) the standard LHD and (b) the LID configurations with $R_{\text{ax}}=3.6$ m and $B_t=1.5$ T. Amplitudes of observed MHD modes are normalized by $B_t\times 10^{-5}$.

Figure 11 shows a comparison between the discharges in the LID and standard LHD configurations at $R_{\text{ax}}=3.6$ m and $B_t=1.5$ T. $\langle\beta_{\text{dia}}\rangle$ in the LID configuration is defined by using the plasma boundary measured with the T_e profile, as shown in Fig. 10. Almost the same $\langle\beta_{\text{dia}}\rangle$'s of 1.5% have been achieved in both discharges, although the heating power and electron density are different. In the standard configuration, three NBIs are applied up to 1.2 s and then one NBI is turned off, and the absorbed power at 1.1 s is 9.9 MW. Two neutral beams are injected to the LID plasma, and $\langle\beta_{\text{dia}}\rangle$ increases with n_e. The total absorbed power of NBI at 1.9 s is 6.7 MW. In the standard LHD configuration, the $\iota/2\pi\geqslant 1$ resonant modes such as $m/n=1/1$ and $3/4$ are dominantly observed and rotate in the electron diamagnetic direction. The $m/n=1/1$ mode exponentially grows with $\langle\beta_{\text{dia}}\rangle$, as shown in Fig. 9, and the amplitudes of the $\iota/2\pi>1$ resonant modes also increase with $\langle\beta_{\text{dia}}\rangle$. Especially, they were enhanced after the *L-H* transition at $\langle\beta_{\text{dia}}\rangle$ of more than 2%.[4] On the other hand, in the LID configuration, the $\iota/2\pi\geqslant 1$ resonant modes are completely suppressed in spite of the same $\langle\beta_{\text{dia}}\rangle$ as in the standard LHD configuration. The $m/n=3/2$ modes excited inside the $\iota/2\pi=1$ surface are dominantly observed because the pressure gradient, which is

formed inside the $m/n=1/1$ island, is steeper than the standard case. However, these modes are not expected to be crucial in the high-β regime because of the magnetic well formation as well as the $m/n=2/1$ mode.

An improvement factor of plasma confinement in the standard discharge [Fig. 11(a)] is 1.1 while that in the LID case [Fig. 11(b)] is 1.6. Both values are obtained at maximum $\langle\beta_{\mathrm{dia}}\rangle$. Here the improvement factor is defined as the ratio of global energy confinement time obtained in experiments to that estimated by International Stellarator Scaling 95 (ISS95).[15] The LID discharge seems to have a better confinement than the standard one. However, the improvement factor in the standard configuration is relatively low compared with the previous experiments.[16] One of reasons is the degradation of the confinement due to the increase in the density rather than edge MHD activities. In the Fig. 11(a) discharge, the electron density is about 5×10^{19} m^{-3}, which is quite high compared with the usual operation with $n_e=(2-3)\times10^{19}$ m^{-3}. The large improvement with the LID has not been observed at the higher density.

V. DISCUSSION AND SUMMARY

The high-β plasma production with $\langle\beta_{\mathrm{dia}}\rangle$ of up to 4.1% has been realized with the high heating power in the configuration with the high-aspect ratio, and serious MHD activities have not been observed in this $\langle\beta_{\mathrm{dia}}\rangle$ range. The reduction of the Shafranov shift due to the high aspect ratio is experimentally confirmed, and leads to keeping the high heating efficiency of neutral beams and to the restraint of the helical ripple loss of high energy particles. On the other hand, the MHD theory suggests that the increment of the aspect ratio causes the restraint of magnetic well formation and destabilizes ideal interchange modes.[10] In the experiments, the $m/n=2/1$ mode has been observed in the middle $\langle\beta_{\mathrm{dia}}\rangle$ range of less than 2.5%, and degrades the plasma confinement by about 10% even in the high-aspect-ratio configuration. However, in addition to the spontaneous stabilization in the high-β regime, we can avoid this instability actively by the elimination of the resonance, due to a moderate plasma current or due to selecting the higher aspect ratio configuration. Although the Mercier criterion is one of the useful indices of the destabilization of MHD modes,[2] it cannot be applied as the index of the available operational regime so far. The validity of the linear MHD theory has been investigated through the relationship between the observed pressure gradient and the growth rate estimated by the ideal low-n mode theory in Ref. 17. The quantitative comparison between the linear theory and experiments will be required for the design of helical fusion reactors.

In the high-β regime, several MHD modes in the periphery are excited and spontaneously stabilized in turn when β increases, which may suggest an expansion of the MHD *stable* region of the plasma. The complex structure of the T_e profile such as the flattening around the resonances appears in the high-β regime, and the relation between this structure and mode stabilization has been investigated. There are three possibilities for the interpretation of this phenomenon. The first one is the self-stabilization of the MHD modes due to nonlinear effect.[18] According to this, the pressure profile can be self-organized through the nonlinear evolution of the interchange mode, so that the plasma should attain the high-β regime beyond the linear stability limit for fixed, smooth pressure profiles. The second one is that the rotation of the mode is stopped and the saturated structure appears in the T_e profile. For example, the $m/n=1/1$ mode has the same frequency of about 1 kHz as that in the discharge shown in Fig. 3, but the decrease in frequency like in the so-called locked mode has not been observed. The third possibility is that the profile flattening is caused by the change of the edge magnetic surfaces due to the finite-β effects. Recent theoretical MHD analysis suggests that the disturbance of the edge magnetic field structure due to the finite-β effect ergodizes the magnetic surface and/or generates the high-n magnetic island.[19] In addition, the "self-heal" phenomena of the magnetic islands have been observed in the high-β regime.[20] Thus, the careful reconstruction of the equilibrium with applying the asymmetrical profile is required for understanding the mechanism of the mode stabilization.

In the limiter and LID experiments, the suppression of the edge MHD modes by the control of pressure gradients is succeeded. These results are useful for not only the identification of pressure driven modes but also clarifying the relationship between the edge mode activities and ergodic magnetic structures in the standard LHD configuration. In the present study, the experiments have been done only in the low-β range, where the affects of MHD activities on plasma confinement are relatively small. Therefore, the same experiments should be done in the high-β regime in the near future.

In summary, the amplitudes of edge MHD modes in the edge region with a magnetic hill configuration grow with the increase in $\langle\beta_{\mathrm{dia}}\rangle$, and they are spontaneously stabilized when $\langle\beta_{\mathrm{dia}}\rangle$ exceeds a threshold value. At the same time, the flattening of electron temperature profile is found around the resonance. The limiter and local island divertor experiments have been performed as attempts to control the edge plasmas, especially, the pressure-driven modes. The stabilization of the edge MHD modes has been realized in both experiments, which shows that their techniques are available for the production of higher-β plasmas without edge MHD activity.

ACKNOWLEDGMENTS

The authors are grateful to worldwide collaborations, and collaborational efforts to perform the LHD project by the Japanese universities and other institutes are greatly appreciated. The authors would like to thank all members of device engineering group for their support and operation of the machine.

[1] K. H. Burrell, M. E. Austin, D. P. Brennan *et al.*, Plasma Phys. Controlled Fusion **44**, A253 (2002).
[2] S. Sakakibara, H. Yamada, K. Y. Watanabe *et al.*, Plasma Phys. Controlled Fusion **44**, A217 (2002).
[3] K. Y. Watanabe, A. Weller, S. Sakakibara *et al.*, Fusion Sci. Technol. **46**, 24 (2004).
[4] K. Toi, S. Ohdachi, S. Yamamoto *et al.*, Nucl. Fusion **44**, 217 (2004).
[5] A. Komori, N. Ohyabu, S. Masuzaki *et al.*, J. Anal. Chem. USSR **241–243**, 967 (1997).

[6]T. Morisaki, S. Masuzaki, A. Komori *et al.*, J. Nucl. Mater. **337-339**, 154 (2004).
[7]A. Komori, T. Morisaki, S. Masuzaki *et al.*, "Edge plasma control by local island divertor in lHD," *Proceedings of the 20th Fusion Energy Conference, Portugal, 2004* (International Atomic Energy Agency, Vienna, to be published).
[8]O. Motojima, K. Ida, K. Y. Watanabe *et al.*, "Confinement and MHD Stability in the Large Helical Device," *Proceedings of the 20th Fusion Energy Conference, Portugal, 2004* (International Atomic Energy Agency, Vienna, to be published).
[9]H. Yamada, N. Ohyabu, K. Y. Watanabe *et al.*, Plasma Phys. Controlled Fusion **44**, A245 (2002).
[10]K. Ichiguchi, O. Motojima, K. Yamazaki *et al.*, Nucl. Fusion **36**, 1145 (1996).
[11]S. Sakakibara, H. Yamada, K. Y. Watanabe *et al.*, Nucl. Fusion **41**, 1177 (2001).
[12]S. P. Hirshman and W. I. van RIJP. Merkel, Comput. Phys. Commun. **43**, 143 (1986).
[13]K. Ichiguchi, Y. Nakamura, M. Wakatani *et al.*, Nucl. Fusion **29**, 2093 (1989).
[14]T. Hayashi, T. Sato, H. J. Gardner *et al.*, Phys. Plasmas **2**, 752 (1995).
[15]U. Stroth, M. Murakami, R. A. Dory *et al.*, Nucl. Fusion **36**, 1063 (1996).
[16]H. Yamada, A. Komori, N. Ohyabu *et al.*, Plasma Phys. Controlled Fusion **43**, 55 (2001).
[17]K. Y. Watanabe, S. Sakakibara, Y. Narushima *et al.*, "Effects of global MHD instability on operational high-β regime in LHD," *Proceedings of the 20th Fusion Energy Conference, Portugal, 2004* (International Atomic Energy Agency, Vienna, to be published).
[18]K. Ichiguchi, N. Nakajima, M. Wakatani *et al.*, Nucl. Fusion **43**, 1101 (2003).
[19]K. Y. Watanabe (private communication).
[20]N. Ohyabu, K. Ida, T. Morisaki *et al.*, Phys. Rev. Lett. **88**, 055005 (2002).